Critical currents in frustrated two-dimensional Josephson arrays

S. P. Benz, M. S. Rzchowski, M. Tinkham, and C. J. Lobb*
Department of Physics and Division of Applied Sciences, Harvard University, Cambridge, Massachusetts 02138
(Received 9 April 1990)

Using the peak in dynamic resistance versus current to indicate the intrinsic critical current I_{c0}, the magnetic-field dependence of I_{c0} in two-dimensional Josephson junction arrays has been inferred from differential resistance measurements at finite voltages. This peak is particularly clear when a magnetic-field-induced vortex superlattice is strongly commensurate with the underlying lattice. At weakly commensurate fields, dV/dI rises sharply at approximately 10% of the zero-field I_{c0}, in qualitative agreement with the prediction of Lobb *et al.* [Phys. Rev. B **27**, 150 (1983)] for the pinning of isolated vortices. New exact calculations of the critical current are presented for the cases of $f=\frac{1}{2}$ and $\frac{1}{3}$ (f is the average number of flux quanta per cell of the array), which agree well with our experimental measurements. Implications of these exact results for the effect of boundary conditions in computer simulations on small arrays are also noted.

I. INTRODUCTION

In defining the critical current of a superconductor, one must distinguish between the intrinsic critical current I_{c0}, which is the maximum supercurrent for which a metastable state exists, and the (lower) current I_{cR}, at which resistance becomes observable because of thermally activated processes. Although I_{cR} has practical importance, it has neither fundamental significance nor a unique value, because it depends on the sensitivity of the experiment that defines it. It is the intrinsic I_{c0} which enters into fundamental analyses, *including the theoretical determination of the onset of resistance.* The relation between I_{c0} and I_{cR} was worked out long ago for single heavily damped Josephson junctions (by Ambegaokar and Halperin)[1] and for one-dimensional filaments (by Langer and Ambegaokar, and McCumber and Halperin).[2] However, this relationship is much less well understood in two-dimensional arrays of Josephson junctions or other weak links, because of the important and complicating role played by flux quanta in the description of an extended system. This type of system is currently attracting much attention as a model system for naturally occurring granular superconductors, particularly the high-temperature superconductors. In this paper we address the issues of critical currents and resistance in such arrays from both experimental and theoretical points of view.

Two-dimensional (2D) arrays of Josephson junctions in zero magnetic field undergo a Kosterlitz-Thouless (KT) transition[3] to an ordered state below a transition temperature T_c. When a magnetic field is applied, vortices of current appear in the array. At magnetic fields where the average number f of flux quanta per unit cell of the array is the ratio p/q of two integers, the lowest-energy state is a spatially periodic one, in which the vortices arrange themselves in an ordered $q\times q$ superlattice that is commensurate with the underlying array of junctions.[4] The transition temperature, $T_c(f)$, and the critical current, $I_{c0}(f)$, for a square array have been shown[4,5] to be periodic for integer changes in f and symmetric about $f=\frac{1}{2}$. Both have their largest values when the vortex superlattice is strongly coupled to the underlying square array, which occurs when f is the ratio of *small* integers, namely when $f=0$, $\frac{1}{4}$, $\frac{1}{3}$, $\frac{1}{2}$, $\frac{2}{3}$, $\frac{3}{4}$, and 1. We will define these fields as "strongly commensurate" fields.

In recent work in this laboratory, the rf response of arrays[6] and the effects of pinning[7] have been investigated experimentally. The analysis of these data depend crucially on knowledge of the Josephson coupling energy E_J of the junctions of the array, or, equivalently, their intrinsic critical currents i_{c0}, because the energy barriers to vortex motion and the characteristic frequency of the overdamped junctions are both proportional to this critical current. In this paper[8] we present experimental measurements of the dynamic resistance at finite voltage as a function of both dc bias current and perpendicular magnetic field (or f) at a temperature far enough below $T_c(f)$ that the effects of thermally induced vortices, domains, and other defects are not important,[9,10] and yet not so low that the flux LI_{c0} per cell has become comparable to Φ_0.[11,12] We discuss how intrinsic unfluctuated critical currents *both for single junctions and for the array* may be extracted from these data by using the analogy with thermal activation of an overdamped particle in a periodic potential. These experimentally determined critical currents will be compared with a new exact analytical calculation of the ground-state critical current for the fully-frustrated case, $f=\frac{1}{2}$, and a precise numerical calculation for $f=\frac{1}{3}$. Finally, we will comment on implications of these exact results for the choice of the type of current feed in simulations of this system using the relatively small arrays that are computationally convenient.

II. SAMPLE FABRICATION AND MEASUREMENT TECHNIQUES

Our two-dimensional arrays consist of 1000×1000 Nb-Cu-Nb proximity-effect junctions. Sample fabrication

is begun by depositing a superconductor–normal-metal bilayer onto a sapphire substrate which has been previously patterned with photoresist to define the dimensions of the array and the measuring leads.[13] The sapphire substrate is cleaned with an rf argon plasma to promote adhesion prior to thermally evaporating 0.35 μm of high-purity copper to form the normal-metal layer. The sample is then moved to a magnetron sputtering machine and mounted on a 60 °F water-cooled substrate holder. The sample is rf-Ar ion etched to remove any oxide that may have formed on the surface of the copper. About 50 nm of copper is removed and then 0.2 μm of niobium is sputtered immediately (within 1 sec) to ensure that a clean interface is formed. Cross-shaped niobium islands are formed by patterning photoresist islands on the bilayer and then reactive ion etching with SF_6 to remove the unwanted niobium between the islands. The islands have a lattice constant a of 10μm and the proximity-effect weak links, consisting of the underlying copper between the islands, are defined by the width (4μm) of the arms of the cross and the separation (2μm) between their tips. Two single junctions with the same geometry as the junctions in the array are concurrently made adjacent to the array on the same substrate. Because the array is square, it has the same normal-state resistance as the single junctions ($R_n \sim 2$ mΩ), determined primarily by the copper.

The samples were mounted in a temperature-controlled, μ-metal shielded, ^{4}He cryostat. A four-point measurement circuit with a lockin amplifier at 45.5 Hz and a battery-powered dc current source was used. A 1:100 transformer was used at the lockin input to improve the impedance match from the low-resistance array. A perpendicular magnetic field was applied to the array using a long copper solenoid. Separate pairs of superconducting bus bars were used to current bias the array and to measure the voltage across it. The dynamic resistance, dV/dI, was measured versus dc current for different magnetic fields and versus field for fixed dc currents. The rms amplitude of the ac current through the sample was always at least 100 times smaller than the measured critical current. All the data in this paper are from an array with $T_c = 3.5$K and measured at $T = 2.09$ K to avoid the effects of thermally excited vortices found near the KT transition temperature. The data were initially plotted on an analog XY recorder and then digitized for computer analysis.

III. EXPERIMENTAL RESULTS AND DISCUSSION

Figure 1 shows the dynamic resistance versus current at several values of f for our 1000×1000 array. In the curve for $f = 0$, a prominent peak appears at about 7 mA, which we will now argue can be used to identify the unfluctuated critical current I_{c0}. For a start, it is plausible on simple physical grounds that a peak in differential resistance should occur (i.e., that the resistive voltage should rise most rapidly) when $I \approx I_{c0}$, since in the absence of thermal fluctuations, the voltage would be zero below I_{c0}, and rise suddenly to a finite value above I_{c0}. For *single* overdamped[14] junctions, this identification of i_{c0} with the position of the peak follows rigorously from

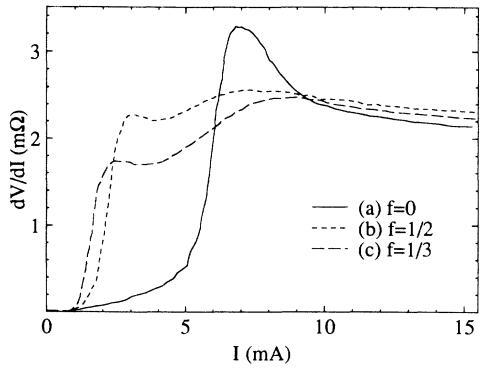

FIG. 1. Dynamic resistance vs current for a 1000 by 1000 array at $T = 2.09$ K for three commensurate perpendicular magnetic fields: (a) $f = 0$, (b) $f = \frac{1}{2}$, and (c) $f = \frac{1}{3}$. The rms lockin current was 30 μA. The data were taken on an XY recorder and then manually digitized for computer analysis.

the work of Ambegaokar and Halperin[1] (AH), from which it has been shown[15] that a peak in dv/di versus i occurs at a current which is within a few percent of i_{c0}, the critical current in the absence of fluctuations, so long as fluctuation effects are small enough that the peak value of dv/di is at least 1.5 times larger than the high-current limiting value of dv/di. Thus, for *single* junctions the position of this peak is a very good measure of the unfluctuated critical current.

In 2D arrays, there are many more degrees of freedom than in single junctions. Insofar as an applied field imposes a strongly commensurate vortex superlattice which moves rigidly, there is a strong analogy with the AH single junction analysis. However, the rounding of the current-voltage curves at finite temperature arises also from more complicated two-dimensional fluctuations, such as thermally-activated vortex-pair unbinding, individual vortex motion, and other excitations that lead to nonrigid motion of the vortex superlattice. In the absence of a quantitative theory for this 2D case, we simply *assume* that the measured current where the dynamic resistance of the array is a maximum gives a good estimate of the intrinsic critical current $I_{c0}(T)$ of the array. This is probably a good assumption at the measured temperatures, where $T \ll T_c$ and the number of vortex-pair excitations is small. In zero field, this I_{c0} should be related to the single junction critical current, i_{c0}, simply by $I_{c0} = Mi_{c0}$, where $M = 1000$ is the number of junctions in parallel across the width of the array perpendicular to the current. This conclusion is supported by the fact that $i_{c0} = I_{c0}/M$ agrees within 10% with the i_{c0}'s for the two single junctions on the same substrate, measured in the same way. Further justification for using the peak to determine the unfluctuated array critical current follows from noting that the temperature dependence of the inferred array critical current follows the exponential temperature dependence expected for the intrinsic critical current of a single weakly coupled SNS junction.[16]

It is important to note that the array current I_{cR} defined experimentally as the lowest current giving measureable voltage would give a much poorer estimate of

the *unfluctuated* critical current I_{c0}, because the relation between this I_{cR} and the intrinsic I_{c0}, is strongly dependent on the voltage criterion used and on the ratio of the relevant energy barrier to the temperature.

The dynamic resistance versus current was found to vary greatly for different magnetic fields. Figure 1 shows dV/dI versus I for two commensurate magnetic fields, $f=\frac{1}{2}$ and $\frac{1}{3}$, at the same temperature as the $f=0$ curve. The dV/dI versus I curves for $f=\frac{2}{3}$ and 1 (not shown) are nearly identical to the $f=\frac{1}{3}$ and $f=0$ curves, respectively, thereby establishing the symmetry about $f=\frac{1}{2}$ and the periodicity for integer changes in f. For these strongly commensurate magnetic fields, weaker local peaks in dV/dI occur at currents lower than that for the peak in zero field ($f=0$). By analogy with the single junction and $f=0$ cases, we associate these peaks with the intrinsic unfluctuated critical currents for these f values, $I_{c0}(f)$. For other commensurate fields, where the vortex superlattice is less strongly coupled to the array, such as $f=\frac{1}{4}$, $\frac{1}{6}$, etc., we observe similar structure in the dynamic resistance at low currents, but the peaks are even less pronounced and have become only rounded features, making it very difficult to make a quantitative inference of i_{c0}. This structure will be discussed below in more detail.

To obtain information about the dynamic resistance at fields other than the "strongly commensurate" fields, the magnetoresistance (dV/dI versus f) was measured at temperatures well below $T_c(f)$ for various fixed bias currents; three such curves are shown in Fig. 2. Curve (a) shows the behavior at a current only slightly above the current at which the dynamic resistance first becomes measurable. Relative minima in the magnetoresistance are observed for $f=0$, $\frac{1}{6}$, $\frac{1}{4}$, $\frac{1}{3}$, $\frac{1}{2}$, $\frac{2}{3}$, $\frac{3}{4}$, $\frac{5}{6}$, and 1, each corresponding to a field where the vortex superlattice is strongly commensurate with the junction array. The symmetry around $f=\frac{1}{2}$ is again apparent. As the bias current is increased from $\sim I_{cR}$, the relative *minima* evolve into relative *maxima*, beginning with the least strongly commensurate fields which have the lowest values of $I_{c0}(f)$. This is shown in curve (b) of Fig. 2 [taken at twice the current as curve (a)], in which weak relative maxima appear near all the commensurate fields except for $f=0$, $\frac{1}{2}$, and 1, which are the *most* strongly commensurate fields. These subtle relative maxima in the magnetoresistance occur near the same currents and fields where the peaks are found in the dV/dI versus I curves. Curve (c), taken at still higher current, 2.79 mA, shows the dramatic reversal of the dip at $f=\frac{1}{2}$ into a maximum, which occurs for $I\sim I_{c0}(f=\frac{1}{2})$. This structure is best revealed when the data are plotted in three dimensions as in Fig. 3, which shows dV/dI as a function of both magnetic field and bias current.

Figure 3 consists of *experimental data*, digitized from dV/dI versus f curves (including those in Fig. 2) at small increments of dc current. The dV/dI versus I curves can be reproduced from this data, as can be seen by comparing the nearest edge of the 3D plot ($f=0$) with curve (a) in Fig. 1. The symmetry about $f=\frac{1}{2}$ is again apparent from this graph; similar structure is observed

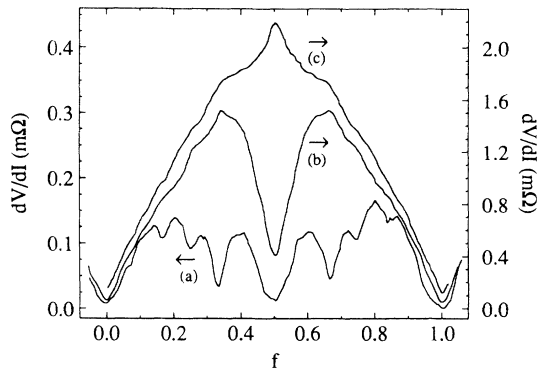

FIG. 2. Magnetoresistance at $T=2.09$ K for three different dc bias currents: (a) 0.92 mA, (b) 1.84 mA, and (c) 2.79 mA. Note that the left and right vertical scales differ by a factor of 5. Minima in the dynamic resistance coincide with magnetic fields where the vortex superlattice is commensurate with the array of junctions, namely $f=0$, $\frac{1}{6}$, $\frac{1}{4}$, $\frac{1}{3}$, $\frac{1}{2}$, $\frac{2}{3}$, $\frac{3}{4}$, $\frac{5}{6}$, and 1.

between all integer f. [At substantially higher fields (not shown), though, a reduction in the array critical current is observed, due to field penetration into the single junctions.[17] The critical current is approximately zero at a field of $f=9$, which accurately corresponds to one quantum of flux threading each junction. This, however, is not a substantial effect for the small fields, $0<f<1$, shown in Fig. 3.]

A number of important features are apparent in this plot, all of which can be explained qualitatively by considering the array of junctions to generate a periodic 2D "egg-carton" potential, in which, given thermal activa-

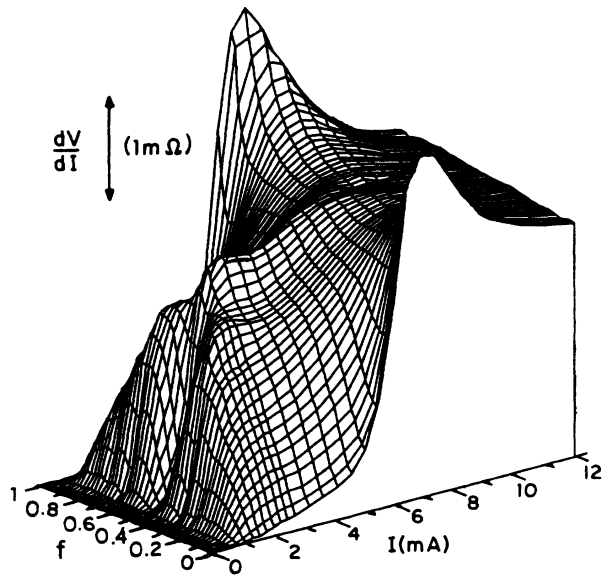

FIG. 3. *Experimental* data showing the detailed dependence of the dynamic resistance on both dc bias current and perpendicular magnetic field. The data were taken from dV/dI vs f curves at fixed bias currents, digitized and then interpolated to retrieve points at convenient intervals along the f and current axes.

tion,[18] field-induced vortices can move in response to a Lorentz force proportional to the dc bias current. At "strongly commensurate" fields, the vortex superlattice is strongly coupled to the array and not easily depinned. In Fig. 3 it is seen that the peaks in the dynamic resistance indicating critical current values are associated with the commensurate fields, and that the heights of the peaks get smaller for the less "strongly commensurate" fields, starting from $f=0$ and 1, to $f=\frac{1}{2}$, and then to $f=\frac{1}{3}$, etc. We identify the current at these peaks, like those shown in Fig. 1, with the depinning current of the vortex superlattices from the periodic 2D potential.[19] This identification is reasonable because thermally activated motion of vortices in a periodic potential due to a Lorentz force is qualitatively similar, as shown explicitly by Rzchowski *et al.*,[7] to the thermally activated behavior for a single junction as described by AH. More simply, it is plausible on physical grounds that the underlying critical current should be found at the current at which the resistive voltage increases most steeply, as mentioned earlier for $f=0$. If we choose the positions of the peaks as estimates for the array critical current for these magnetic fields, and compare with the zero field case, we find

$$I_{c0}(f=\tfrac{1}{2})\approx 0.42 I_{c0}(f=0)$$

and

$$I_{c0}(f=\tfrac{1}{3})\approx 0.34 I_{c0}(f=0)\ .$$

As we shall see, these critical currents are in reasonable agreement with theoretical critical currents discussed in Sec. IV of this paper.

The curves in Fig. 2 can now be explained. The Lorentz force, due to the dc current, has the effect of tilting the 2D "egg-carton" potential. The energy barriers to motion of the vortex superlattice differ for the different commensurate fields, depending on the coupling strength between the vortex superlattice and the array. For fields f near the "strongly commensurate" fields f_c it has been suggested[4,7] that unpaired, field-induced vortices or some other form of defects dominate the dynamic resistance as they are thermally activated and driven by the Lorentz force. Since the number of these defect vortices is proportional to $|f-f_c|$, the resistance rises approximately linearly on either side of the minimum at f_c. The small *maxima* in the magnetoresistance at commensurate fields f_c, particularly in the higher current plots (b) and (c), signify that the bias current is very close to the depinning current, $I_{c0}(f_c)$, for those particular commensurate fields, i.e., the energy barriers to vortex motion have been reduced to near zero by the current.

At very high currents all the barriers to vortex motion are reduced to zero and the array is in a flux-flow regime where all the field-induced vortices are depinned and flowing down the tilted 2D potential. This regime can be seen in Fig. 3 for fixed currents between the $f=\frac{1}{2}$ and $f=0$ critical currents, where the dynamic resistance is rising nearly linearly as a function of field between $f=0$ and $f=\frac{1}{2}$ as would be expected in the flux-flow regime of a type-II superconductor. The slope of this line, $\sim 2.3R_n$ is in good agreement with the value of $2R_n$ obtained by considering the viscous drag on each vortex.[7] Between $f=\frac{1}{2}$ and $f=1$ the dynamic resistance *decreases* linearly because now vortices of the opposite sign dominate, and their number is decreasing as $f=1$ is approached. At currents far above the zero-field critical current, the behavior of the array is dominated by the normal shunt resistance of the copper in the junctions, so the dynamic resistance is essentially independent of both current and magnetic field.

The next interesting feature is that the dynamic resistance is not appreciable for any value of f when the dc current

$$I \le 0.1 I_{c0}(f=0)\approx 0.7\ \text{mA}\ .$$

We believe this feature is related to the pinning energy of individual vortices in the array as calculated by Lobb *et al.*,[20] $E_B=0.2E_J$. As verified by simulations,[7,21] the current required to depin a solitary vortex in the absence of thermal activation is $0.1i_{c0}$ per junction, which is in agreement with our observed total array current of $0.1I_{c0}(f=0)$. The fact that we observe this same minimum depinning current for *all* fields, and not just for small field near $f=0$, suggests that the depinning current for field-induced defects is $\sim 0.1 i_{c0}$ per junction near other f_c values as well. The differential resistance peak associated with the depinning of these defects is very small because the dissipation due to the motion of a small number of defects, $\propto |f-f_c|R_n$ is very small, thus forcing us to use a resistive onset criterion in this case. At much lower temperatures this zero-dissipation plateau region becomes larger due to self-induced field effects in the array.[11]

Theoretical estimates for the critical currents of an array in commensurate magnetic fields have been obtained by a number of different methods. Teitel and Jayaprakash[4] used Monte Carlo simulations with a twisted-phase method to induce a dc current in order to determine the zero-temperature ground-state critical current for various fields. Shih and Stroud[5] used a molecular-field approximation with the twisted-phase method and found similar critical currents. From their published data we find their critical current estimates for $f=\frac{1}{2}$ and $f=\frac{1}{3}$ to be

$$I_c(f=\tfrac{1}{2})/I_c(f=0)\approx 0.41\pm 0.01$$

and

$$I_c(f=\tfrac{1}{3})/I_c(f=0)\approx 0.26\pm 0.01\ .$$

We have made exact critical current calculations for both of these fields by calculating the current dependence of the gauge invariant phase difference across each junction. This method is discussed in detail for $f=\frac{1}{2}$, and sketched for $f=\frac{1}{3}$, in Sec. IV of this paper. From these calculations we find analytically

$$I_{c0}(f=\tfrac{1}{2})/I_{c0}(f=0)=\sqrt{2}-1=0.41421$$

(as was found numerically by Halsey)[22] and

$$I_{c0}(f=\tfrac{1}{3})/I_{c0}(f=0)=0.26789 \ .$$

The results of the simulations mentioned above are in excellent agreement with these exactly calculated values. For convenience of comparison, the measured, exactly calculated, and simulated critical current ratios are collected in Table I.

The estimated critical current ratio for $f=\frac{1}{2}$ from our experimental measurements (~ 0.42) is also in excellent agreement with the exact critical current, but for $f=\frac{1}{3}$ the peak in the dynamic resistance appears at a current (~ 0.34) that exceeds the theoretical value. The position of the rounded peaks in Fig. 3 for other less strongly commensurate fields also appear to overestimate $I_{c0}(f)$ compared to the simulated values for $T=0$.[4,5] A possible reason for this discrepancy is that the peaks are more rounded for the less strongly commensurate fields, probably due to more thermal activation over their lower energy barriers. In the AH model, for smaller values of $\gamma=E_B/kT=\hbar i_{c0}/ekT$ the peak in dv/di is suppressed in magnitude and shifts toward currents higher than i_{c0}. Despite their difference in detail, thermal excitations in arrays may cause an analogous change in the position of this peak, thus yielding an overestimate of $I_{c0}(f)$ for the less strongly commensurate fields. Nonuniformities in the array may also contribute to the rounding of these peaks because at the less strongly commensurate fields the vortices interact more weakly due to the larger superlattice cell size, and thus they may be more susceptible to variations in junction coupling energies and other nonuniformities.

IV. ANALYTIC SOLUTIONS FOR $f=\frac{1}{2}$ and $f=\frac{1}{3}$

We have made an exact calculation of the critical current for the $f=\frac{1}{2}$ ground state using periodicity and other symmetry arguments to restrict the number of independent gauge-invariant phase differences across the junctions in an infinite array. In our solution, we assume that, as for the zero-current ground state, the current-carrying ground state is made up of vortex superlattice cells of size 2×2 junctions, and that the phase differences deform continuously in response to a net imposed current until the intrinsic critical current is reached, above which no static solutions exist. This ground-state configuration is shown in Fig. 4, where the gauge-invariant phase differences across the four non-equivalent junctions are denoted by α, β, β', and γ. For zero net current, all of these phases are equal to $\pi/4$. A net current applied from left to right will break the symmetry of the ground state, so that α and γ will have different values. If there is no net current in the vertical direction, symmetry requires that $\beta=\beta'$.

TABLE I. Comparison between measured, exactly calculated, and numerically simulated (Refs. 4 and 5) critical currents.

f	$I_c(f)/I_c(0)\|_{\text{meas}}$	$I_c(f)/I_c(0)\|_{\text{exact}}$	$I_c(f)/I_c(0)\|_{\text{sim}}$
0	1	1	1
$\frac{1}{2}$	0.42±0.02	0.414 214	0.41±0.01
$\frac{1}{3}$	0.34±0.02	0.267 89	0.26±0.01

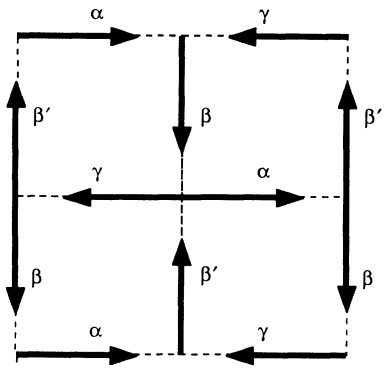

FIG. 4. Ground state 2×2 superlattice unit cell for $f=\frac{1}{2}$, showing the positions of the gauge-invariant phases, $\alpha,\beta',\beta,\gamma$, used to accommodate a net dc bias current in the horizontal direction. By symmetry, β' must equal β when there is net current in the vertical direction. The shaded arrows represent ground-state supercurrents across the junctions and have equal magnitude $i_{c0}\sqrt{2}$ for zero dc bias. The lines between the vertices correspond to the junctions between the superconducting islands.

With these assumptions we can write down the following constraining equations. For $f=\frac{1}{2}$, fluxoid quantization requires that

$$\alpha+\gamma+2\beta=\pi \pmod{2\pi} \ . \tag{1}$$

Current conservation at each node in the array is satisfied if

$$\sin\alpha+\sin\gamma=2\sin\beta \ . \tag{2}$$

Finally, the average net current per junction in the horizontal direction, normalized to the single junction critical current, is

$$i/i_{c0}=\tfrac{1}{2}(\sin\alpha-\sin\gamma) \ . \tag{3}$$

Solving these equations for the net current as a function of the total gauge-invariant phase difference across the 2×2 cell parallel to the current, $\varphi=\alpha-\gamma$, we find

$$\frac{i}{i_{c0}}=\frac{\sin\varphi}{(6+2\cos\varphi)^{1/2}}=\frac{\sin(\varphi/2)}{[1+\sec^2(\varphi/2)]^{1/2}} \ . \tag{4}$$

The maximum current per junction that can be carried in this state is

$$i_{c0}(f=\tfrac{1}{2})=(\sqrt{2}-1)i_{c0} \ ,$$

as can be found by differentiating this expression; this occurs for

$$\varphi=2\sin^{-1}(2-\sqrt{2})^{1/2}\approx 99.88^\circ \ .$$

It is interesting to note that Eq. (4) describes a current-phase relation $I(\varphi)$ that is similar to the single-junction current-phase relation $i=i_{c0}\sin\varphi$ except that now φ denotes the total gauge-invariant phase across the 2×2 vortex superlattice unit cell, and the maximum supercurrent is only $(\sqrt{2}-1)i_{c0}$ per junction, or twice that (i.e.,

$2i_{c0}(f=\frac{1}{2})=0.828\,43i_{c0}$) per 2×2 cell. This current-phase relation for the 2×2 cell is compared with that for a single junction in Fig. 5.

The gauge-invariant phases and hence the currents for each of the junctions can be worked out from this solution, with the following results.[23]

$$\sin\alpha=[1+\sec^2(\varphi/2)]^{-1/2}[1+\sin(\varphi/2)]\ , \tag{5a}$$

$$\sin\beta=[1+\sec^2(\varphi/2)]^{-1/2}\ , \tag{5b}$$

$$\sin\gamma=[1+\sec^2(\varphi/2)]^{-1/2}[1-\sin(\varphi/2)]\ . \tag{5c}$$

The sign ambiguity of the square root is resolved by imposing a requirement of continuity.

We have carried out similar (but more intricate) calculations for the $f=\frac{1}{3}$ ground state. Here one must determine five independent gauge-invariant phase differences within the 3×3 cell, compared to three in the 2×2 cell for $f=\frac{1}{2}$. Although we were not able to find an analytic expression for the maximum supercurrent per junction, it was found numerically to be $i_{c0}(f=\frac{1}{3})=(0.267\,89)i_{c0}$. Referred to the 3×3 superlattice cell, the maximum supercurrent is three times this (i.e., $3i_{c0}(f=\frac{1}{3})=0.803\,67\ i_{c0}$), and occurs at a gauge-invariant phase difference of about 105.23°. The current-phase relation for the $f=\frac{1}{3}$ (3×3) superlattice unit cell was calculated numerically and is also plotted in Fig. 5.

Comparing the three exact solutions in Fig. 5, for $f=0$, $\frac{1}{2}$, and $\frac{1}{3}$, we note that the maximum supercurrent *per superlattice cell* drops only from 1 to 0.828 to 0.804,

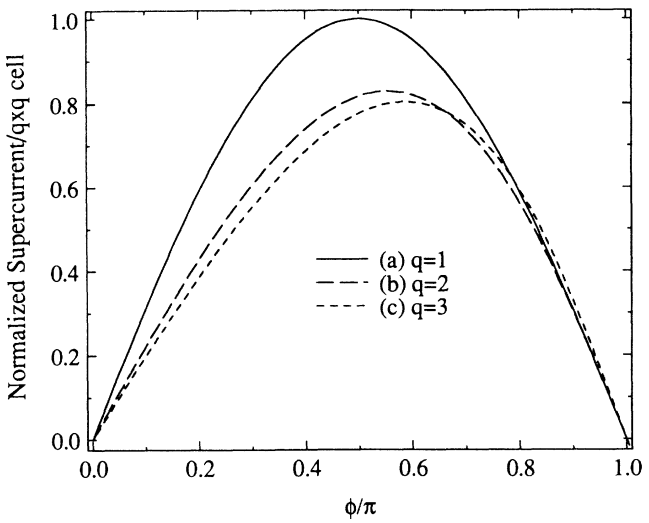

FIG. 5. Comparison of current-phase relation for a single junction, for a 2×2 superlattice cell for $f=\frac{1}{2}$, and for a 3×3 cell for $f=\frac{1}{3}$. The normalized supercurrent per $q\times q$ cell is defined as $q\cdot i(f)/i_{c0}$. The maximum values (0.828 and 0.804) of the curves for $f=\frac{1}{2}$ and $\frac{1}{3}$ correspond to 0.414 and 0.268 per junction as explained in the text. The gauge-invariant phase difference φ occurs across a single junction for $f=0$, but is distributed over two or three junctions in series in the 2×2 or 3×3 cells, respectively. Only half of a complete cycle is shown, to allow detailed features to be more clearly seen.

and that this maximum occurs at a gauge-invariant phase difference *per superlattice* cell that increases only from 90° to 100° to 105°. Thus, the effect of the superlattice on the macroscopic response of the array is a sort of renormalization, in which each $q\times q$ superlattice cell can be approximately replaced by a 1×1 cell in an array with q-fold larger lattice interval, but rather similar maximum supercurrent per $q\times q$ unit cell, $q\cdot i_{c0}(f=p/q)$, and an approximately sinuoidal current-phase relationship.

These exact solutions have implications for computer simulations since they show that the total supercurrent due to the dc bias and the field-induced vortices is not the same for adjacent junctions. If uniform currents are imposed at the boundaries in simulations, the gauge-invariant phase differences across junctions near these edges are distorted from their optimal current-carrying state, resulting in a reduced critical current. For example, with uniform current injection, the zero-temperature critical current per junction for the $f=\frac{1}{2}$ ground state was found to be $i_{c0}(f=\frac{1}{2})=0.35i_{c0}$.[24,25] This is substantially lower than the exact calculated value $(\sqrt{2}-1)\approx0.414$ for an infinite array. As an alternative to uniform current injection, Free *et al.*[25] used currents at the boundaries which were determined from the exact calculations for the periodic $f=\frac{1}{2}$ state, described above in Eq. (5). With periodic boundaries perpendicular to the current and this current injection method, the array behaved as though it were part of an infinite array; the supercurrents in the array were not distorted near the current injection nodes, and the correct ground-state critical current $(\sqrt{2}-1)$ was reproduced.

The experimental arrays discussed above were very large, 1000 by 1000 junctions, had free boundaries on the edges parallel to the current and used superconducting bus bars to inject the current. Arrays fed by normal-metal electrodes configured to inject the current approximately uniformly were also measured and found to display essentially the same dynamic resistance behavior as the arrays with bus bars. We conclude that the experimental arrays are so large that their measured properties are essentially independent of their boundary conditions including the method of current injection, since the few affected rows of junctions at the edge of the array contribute a voltage that is less than one percent of that given by a feature involving the bulk of the array. Accordingly, their measured properties resemble those of an infinite array. On the other hand, since simulations are limited to much smaller arrays, the boundary conditions are more important.

V. CONCLUSION

Systematic measurements of the dynamic resistance of a 2D square array of Josephson junctions have shown it to be a complicated function of both bias current and perpendicular magnetic field. We have consistently explained the major features of this dynamic resistance within a model of the motion of strongly commensurate vortex superlattices in the 2D egg-carton pinning potential of the junction array. This model enabled us to make experimental estimates of the *intrinsic* critical current of

the array in commensurate magnetic fields, which we find to be in quite good agreement with exact theoretical values. The results of the exact calculations for $f=\frac{1}{2}$ and $\frac{1}{3}$ superlattice states suggest the conceptual usefulness of a renormalized array picture. This work complements previous investigations of the resistive dissipation in Josephson junction arrays in zero field near the Kosterlitz-Thouless transition temperature and near the phase transition temperatures for the commensurate magnetic fields. Taken as a whole, these investigations present a fairly complete and unified picture of the dc properties of 2D Josephson junction arrays over a wide range of temperature, current, and magnetic field.

ACKNOWLEDGMENTS

This research was supported in part by National Science Foundation Grant No. DMR-89-20490 and DMR-89-12927, Office of Naval Research Grant No. N00014-89-J-1565, and Joint Services Electronics Program Grant No. N00014-89-J-1023.

---

*Present address: Department of Physics, University of Maryland, College Park, Maryland 20742.

[1]V. Ambegaokar and B. I. Halperin, Phys. Rev. Lett. **22**, 1364 (1969).

[2]J. S. Langer and V. Ambegaokar, Phys. Rev. **164**, 498 (1967); D. E. McCumber and B. I. Halperin, Phys. Rev. B **1**, 1054 (1970).

[3]J. M. Kosterlitz and D. J. Thouless, J. Phys. C **6**, 1181 (1973); D. J. Resnick, J. C. Garland, J. T. Boyd, S. Shoemaker, and R. S. Newrock, Phys. Rev. Lett. **47**, 1542 (1981); David W. Abraham, C. J. Lobb, M. Tinkham, and T. M. Klapwijk, Phys. Rev. B **26**, 5268 (1982).

[4]S. Teitel and C. Jayaprakash, Phys. Rev. Lett. **51**, 1999 (1983).

[5]W. Y. Shih and D. Stroud, Phys. Rev. B **28**, 6575 (1983); **32**, 158 (1985).

[6]S. P. Benz, M. S. Rzchowski, M. Tinkham, and C. J. Lobb, Phys. Rev. Lett. **64**, 693 (1990).

[7]M. S. Rzchowski, S. P. Benz, M. Tinkham, and C. J. Lobb, Phys. Rev. B **42**, 2041 (1990).

[8]A preliminary account of this work was given by S. P. Benz, M. S. Rzchowski, M. Tinkham, C. J. Lobb, and G. O. Zimmerman, Bull. Am. Phys. Soc. **34**, 845 (1989).

[9]The magnetoresistance and *I-V* characteristics of overdamped arrays have previously been measured only very close to $T_c(f=0)$: M. Tinkham, D. W. Abraham, and C. J. Lobb, Phys. Rev. B **28**, 6578 (1983); R. K. Brown and J. C. Garland, *ibid.* **33**, 7827 (1986); K. N. Springer and D. J. Van Harlingen, *ibid.* **36**, 7273 (1987); D. J. Resnick, R. K. Brown, D. A Rudman, J. C. Garland, and R. S. Newrock, in *Proceedings of the 17th International Conference on Low Temperature Physics* (North-Holland, Amsterdam, 1984), p. 739; D. Kimhi, F. Leyvraz, and D. Ariosa, Phys. Rev. B **29**, 1487 (1984); J. M. Gordon, A. M. Goldman, M. Bushan, and R. H. Cantor, Jpn. J. Appl. Phys. **26**, 1425 (1987).

[10]Arrays of underdamped junctions exhibit hysteretic *I-V* curves and behave much differently than overdamped arrays, although the field modulation of the subgap resistance, $R_0(f)$ behaves similarly to the magnetoresistance in overdamped arrays: Richard F. Voss and Richard A. Webb, Phys. Rev. B **25**, 3446 (1982); R. A. Webb, R. F. Voss, G. Grinstein, and P. M. Horn, Phys. Rev. Lett. **51**, 690 (1983); H. S. J. van der Zant, C. J. Muller, H. A Rijken, B. J. van Wees, and J. E. Mooij, Physica B **152**, 56 (1988).

[11]This is analogous to self-induced fields affecting the magnetic field modulation of the critical current in a dc SQUID: M. Tinkham, *Introduction to Superconductivity* (McGraw-Hill, New York, 1975; reprinted by Krieger, Florida, 1985), p. 215–216.

[12]At these temperatures the penetration depth for a perpendicular magnetic field is smaller than the array size. However, in the highly resistive regime of our measurements, the currents flow uniformly, and this is not an important effect.

[13]M. G. Forrester, Hu Jong Lee, M. Tinkham, and C. J. Lobb, Phys. Rev. B **37**, 5966 (1988).

[14]An overdamped junction has $\beta_c=2ei_cR^2C/\hbar<1$, where C is the capacitance of the junction. Our single junctions have negligible capacitance so that $\beta_c \ll 1$.

[15]C. M. Falco, W. H. Parker, S. E. Trullinger, and P. K. Hansma, Phys. Rev. B **10**, 1865 (1974).

[16]P. G. DeGennes, Rev. Mod. Phys. **36**, 225 (1964).

[17]M. Tinkham, *Introduction to Superconductivity* (McGraw-Hill, New York, 1975; reprinted by Krieger, Florida, 1985), p. 199.

[18]AC response measurements at various temperatures by Ch. Leeman, Ph. Lerch, G.-A. Racine, and P. Martinoli, Phys. Rev. Lett. **56**, 1291 (1986), have shown effects of thermal activation on pinning.

[19]Our model assumes that the array is uniform and that the entire superlattice depins and moves across the array. For arrays with nonidentical junctions or some other form of disorder, the motion may be more complex, including effects such as vortex lattice shear. At higher temperatures close to the $T_c(f)$ the motion of domains or other defects will contribute to dissipation and may destroy the superlattice.

[20]C. J. Lobb, David W. Abraham, and M. Tinkham, Phys. Rev. B **27**, 150 (1983).

[21]J. P. Straley, Phys. Rev. B **38**, 11 225 (1988); K. H. Lee, J. S. Chung, and D. Stroud, in *Workshop on Relaxation and Related Phenomena in Complex Systems, Torino, Italy, 1989,* edited by A. Campbell and C. Giovannella (Plenum, New York, 1989).

[22]T. C. Halsey, Phys. Rev. B **31**, 5728 (1985). In this paper, results for I_{c0} equivalent to ours were found numerically by considering the stability of "staircase states."

[23]The fact that α, β, and γ depend only on $\varphi/2$, implies that their periodicity in φ is over 4π, while (4) shows that the *average* net current per junction is periodic over 2π. This difference reflects an internal period doubling in the case of ac drive as found in the "fractional giant Shapiro steps" at $f=\frac{1}{2}$ reported by Benz *et al.* (Ref. 6) and simulated by Free *et al.* (Ref. 25).

[24]K. K. Mon and S. Teitel, Phys. Rev. Lett. **62**, 673 (1989); J. S. Chung, K. H. Lee, and D. Stroud, Phys. Rev. B **40**, 6570 (1989).

[25]J. U. Free, S. P. Benz, M. S. Rzchowski, M. Tinkham, C. J. Lobb, and M. Octavio, Phys. Rev. B **41**, 7267 (1990).